ChemInform Abstract: High-Pressure Transformation in the Cobalt Spinel Ferrites.

Article *in* Journal of Solid State Chemistry · February 2015

DOI: 10.1016/j.jssc.2014.09.028

High-pressure transformation in the cobalt spinel ferrites

J. Blasco[1], G. Subías[1], J. García[1], C. Popescu[2] and V. Cuartero[3]

[1]Instituto de Ciencia de Materiales de Aragón and Departamento de Física de la Materia Condensada, Consejo Superior de Investigaciones Científicas y Universidad de Zaragoza, 50009 Zaragoza, Spain.

[2]CELLS-ALBA Synchrotron Light Facility, Ctra. BP1413 km 3.3, 08290 Cerdanyola del Vallès, Barcelona, Spain

[3]European Synchrotron Radiation Facility, F-38043 Grenoble Cedex 9, France

Corresponding author:

J. Blasco

I.C.M.A. Departamento de Física de la Materia Condensada

C.S.I.C.-Universidad de Zaragoza

50009 Zaragoza (Spain)

e-mail:jbc@posta.unizar.es

Fax:+34-976-761229

Abstract

We report high pressure angle-dispersive x-ray diffraction measurements on $Co_xFe_{2-x}O_4$ (x=1, 1.5, 1.75) spinels at room temperature up to 34 GPa. The three samples show a similar structural phase transformation from the cubic spinel structure to an analogous post-spinel phase at around 20 GPa. Spinel and post-spinel phases coexist in a wide pressure range (~20 – 25 GPa) and the transformation is irreversible. The equation of state of the three cubic spinel ferrites was determined and our results agree with the data obtained in related oxide spinels showing the role of the pressure-transmitting medium for the accurate determination of the equation of state.

Measurements releasing pressure revealed that the post-spinel phase is stable down to 4 GPa when it decomposes yielding a new phase with poor crystallinity. Later compression does not recover either the spinel or the post-spinel phases. This phase transformation induced by pressure explains the irreversible lost of the ferrimagnetic behaviour reported in these spinels.

1.- Introduction

Mixed transition-metal oxides with cubic spinel structure (AB_2O_4; A tetrahedral and B octahedral sites) have been widely studied in the past because of its wide spread over the Earth and its use in different technological applications due to their magnetic and electric properties that can be modulated by changing the cationic composition [1]. Because of spinel density is relatively low since the presence of occupied tetrahedral sites prevents further compaction of the oxygen sublattice, lattice compression lead to structural transitions [2-4] which strongly affects their electrical and magnetic properties [5-7]. Pioneering studies on the high pressure structural properties of cubic spinels were focused in understanding the behavior of Earth constituents in the crust and mantle [8] revealing that upon compression the spinels can adopt orthorhombic structures denoted as postspinels. The structure and properties of postspinels are still under debate. The reason is the great similarity of the possible high-pressure phases that can be isostructural to $CaMn_2O_4$, $CaFe_2O_4$ or $CaTi_2O_4$ [4]. The three phases have orthorhombic cells with similar lattice parameters and the transformation from spinel to one of these phases imply that cations change their coordination from tetrahedral and octahedral to octahedral and dodecahedral, respectively. Consequently, a more compact structure is formed and the phase transition occurs together with a small volume collapse. An example of the ambiguities that appear in the literature is the case of magnetite. High-pressure XRD patterns of Fe_3O_4 have been analyzed using the $CaMn_2O_4$-type [9] and the $CaTi_2O_4$-type [10-11] structures.

Regarding the magnetic properties, one of the most studied compounds are spinel ferrites. An interesting fact observed in these spinel ferrites is that pressure induces the disappearance of magnetism [12,13]. Some authors point out a structural phase transition into a non-magnetic phase stable at high pressure whereas other models argue about the magnetic collapse due to the 3d band widening induced by the pressure [12]. The latter effect decreases the density of states at the Fermi level below the stability limit for ferromagnetism given by the Stoner criterion [14]. Recently we have studied the stability of ferrimagnetism in the $Co_xFe_{3-x}O_4$ (x = 1, 1.5, and 2) family showing pressure-induced transitions above 20 GPa [13]. Our results clearly discard any role of the magnetic collapse in $CoFe_2O_4$ and show that a structural phase transition is intimately correlated with the suppression of the ferrimagnetic order into either paramagnetic or antiferromagnetic high-pressure state. The other spinel ferrites also showed correlated pressure-induced magnetic and structural phase transitions. The high

pressure non-magnetic phase of Co_2FeO_4 was found to be isostructural to the $CaMn_2O_4$-type structure but the ascription of the high-pressure phases for the other two studied ferrites was ambiguous due to the occurrence of texture in the XRD patterns. In this paper we report a new structural study performed on a new set of samples prepared by a sol-gel method, which allows the preparation of more homogeneous samples than standard ceramic procedures. Our aim is to verify if all of these cobalt-iron spinels develop the same type of pressured-induced transitions or there exists some difference depending on their chemical composition.

2.- Experimental section.

Polycrystalline samples of $CoFe_2O_4$, $Co_{1.5}Fe_{1.5}O_4$, and $Co_{1.75}Fe_{1.25}O_4$ were synthesized by a sol-gel method using the citrate route. Stoichiometric amounts of Fe and Co were dissolved in a 0.1 M solution of nitric acid. Then, citric acid and ethylene-glycol were added in a ratio of 4g:2ml per g of the resulting oxide. The solution was heated until the gel formation followed by desiccation. The resulting powder was heated overnight at 650º C. The powders were ground and pressed into pellets. The sintering process was adapted to the chemical composition of the sample. $CoFe_2O_4$ was then sintered at 1100ºC for 48 h in air and cooled down to room temperature. $Co_{1.5}Fe_{1.5}O_4$ and $Co_{1.75}Fe_{1.25}O_4$ were sintered at 1100ºC in the same conditions, but they were slowly cooled (1ºC/min) down to 925ºC and quenched into air to prevent decomposition into two spinel phases [15]. The samples were characterized by x-ray powder diffraction (XRD) using a Rigaku D-system and Cu K_α radiation. The chemical composition of the samples was tested by using the wavelength dispersive x-ray fluorescence spectrometry technique (advant'XP+ model manufactured by ARL). The Fe:Co ratio agreed with the nominal one for all samples. Magnetic measurements were carried out between 5 and 300 K by using a commercial Quantum Design (SQUID). These properties agreed with samples with the right oxygen stoichiometry.

Synchrotron XRD experiments under pressure using a membrane diamond-anvil cell (DAC) were carried out at the beam line MSPD in the ALBA synchrotron [16]. The measurements were performed at room temperature in angle dispersive mode with an incident monochromatic wavelength of 0.4246 Å. Samples were loaded in 130 μm diameter holes of 40 μm thick stainless steel gaskets in DAC with diamond culet sizes of 300 μm. Two ruby grains were loaded with the sample for pressure determination [17].

A mixture of methanol and ethanol (4:1) was used as the pressure-transmitting medium. Diffraction images were recorded on a fast scanning CCD camera (Rayonix SX 165). The image data were integrated using the FIT2D software package [18], and the resulting diffraction patterns were analyzed with the Fullprof program [19].

3.- Results and discussion.

Powder XRD were measured on $Co_xFe_{2-x}O_4$ samples (x=1, 1.25, 1.5, 1.75 and 2) synthesized by the abovementioned sol-gel method at room temperature. All samples were successfully refined as cubic spinel (space group $Fd\bar{3}m$) without sign of the tetragonal distortion reported in ref. 20 for $CoFe_2O_4$ but in agreement with ref. 3 and 21. Figure 1 shows a representative refinement. The lattice parameter decreases with increasing the Co-content with a ratio of -0.13 Å/x in this composition range as can be seen in the inset of Fig. 1. This result agrees with the tabulated ionic radii of Co^{2+}/Fe^{2+} and Co^{3+}/Fe^{3+} as iron cations are always bigger [22].

The samples with x=1, 1.5 and 1.75 were chosen to study the structural changes induced by the pressure in this family of compounds. Figure 2 shows representative diffraction patterns obtained for x=1 and x=1.75 up to 34 GPa. Similar behaviour was observed for the intermediate composition x=1.5. The cubic spinel structure is stable up to ~20 GPa and above this pressure, new diffraction peaks appear in the patterns marking the start of a pressure induced structural phase transition. Below this point, only two features are noticeable, a shift of the peaks in agreement with the unit cell contraction as the pressure increases, and a broadening of the peaks above 10 GPa. The latter is likely to be related with the loss of hydrostatic conditions of the methanol/ethanol mixture above 10 GPa [23,24].

Above 20 GPa, the new peaks grow up as the spinel phase gradually disappears. Both phases coexist in a wide pressure range of around 5-7 GPa. At 30 GPa, only the high pressure phase is present. The patterns are typical of postspinel phases but the width of the diffraction peaks prevent an accurate Rietveld refinement (more parameters to be refined than freedom degrees). We have tested the three models ($CaMn_2O_4$-, $CaFe_2O_4$- and $CaTi_2O_4$-like) with constrains and the results were very similar with identical lattice parameters. We have analysed the data using the $CaTi_2O_4$-like model (space group *Bmmb*) as it has got the least number of free parameters among the three models. Figure 3 compares the pressure dependence of the unit cell volume for the

three compounds. The plots show a strong shrink in the volume at the phase transition with increasing pressure because the postspinel phase is much denser. The volume decrease in our samples ranges between 7.8 and 6.4% in agreement with the data reported for related spinels [10,13].

The pressure dependence of the unit cell volume shows a turning point around 10 GPa. This feature is likely related to the loss of hydrostatic conditions abovementioned. In order to test this point, the P(V) data for the spinel phase of the three compositions were fitted to the second order of the Birch-Murnaghan (BM) equation of state using two ranges of fit: Fitting the data with P≤10 GPa (hereafter denoted as BM10) and fitting the data with P≤23 GP (BM23) which is the highest pressure value where accurate Rietveld refinements can be achieved for the spinel phase. By using results up to 10 GPa (BM10) we minimize the influence of deviatoric stresses in the results. The third-order BM isothermal equation of state is given by [25,26]:

$$P(V) = \frac{3K_0}{2}[\eta^{\frac{7}{3}} - \eta^{\frac{5}{3}}]\{1 + \frac{3}{4}(K'_0 - 4)[\eta^{\frac{2}{3}} - 1]\}$$

Where P and V are measured in GPa and Å^3, respectively. $\eta=V_0/V$ and V_0 stands for the reference volume (usually measured at ambient conditions) whereas K_0 and K_0' are the bulk modulus and its pressure derivative, respectively. In the second-order BM isothermal equation, K'_0 is fixed to 4 [3, 27]. A summary of the elastic constants obtained in these fits are summarized in table I and they are compared with a previous measurement of Co_2FeO_4 [13]. As indicated in this table, significant differences are obtained depending on the range of the fit when the alcohol mixture is used as pressure transmitting medium. Overall the bulk modulus deduced from BM23 is higher than the ones from BM10. The latter values range between 177 and 183 very close to the values reported for $CoFe_2O_4$ [3] and Fe_3O_4 [2] using an optimum pressure transmitting medium like He where hydrostatic conditions are kept up to ~50 GPa [3]. BM23 shows higher values of bulk modulus in agreement with the data reported using non-hydrostatic pressure mediums. This suggests that deviatoric stresses cause a reduction of bulk compressibility (increase of bulk modulus) as has been already found in other compounds [2,28,29]. In this way, the fit of Co_2FeO_4 is very good with smaller standard deviations and similar value of bulk modulus. Figure 4 shows the two kinds of fits emphasizing the difference observed below 10 GPa for $Co_{1.5}Fe_{1.5}O_4$ and the quality of the fit for Co_2FeO_4.

This study complements our previous work [13] showing that all $Co_xFe_{3-x}O_4$ spinels ($1 \leq x \leq 2$) show the same type of pressure-induced transition above 20 GPa. The result is a similar postspinel phase without spontaneous magnetization as the magnetic circular dichroic signal vanishes [13]. The irreversibility of this transition, as shown in Fig. 3, reveals that magnetism is not recovered after releasing the pressure. However, if the structural phase transition is not complete (insufficient pressure), the magnetism decreases in according to the phase transformation.

4. Conclusions.

The pressure dependence of XRD measurements using methanol:ethanol as pressure medium has shown that $CoxFe_{3-x}O_4$ spinels ($1 \leq x \leq 1.75$) have the same pressure transition around 20 GPa. The postspinel phase is similar for all compositions and the transition is irreversible because after releasing the pressure, the postspinel phase is stable down to 4 GPa and then it decomposes. The original spinel phase is not recovered even after several hours at ambient pressure and the postspinel phase is not recovered with a second pressurization. Therefore, the loss of ferrimagnetism in these spinels under pressure is very likely related to strong structural changes including the amorphization and the structural transition to a paramagnetic postspinel phase without spontaneous magnetization.

Our study reveals that the alcohol mixture used in this work as pressure media provides hydrostatic conditions for reliable equations of state up to 10 GPa. Above this pressure the medium is only quasi-hydrostatic. However, the bulk modulus obtained for these cobalt-iron spinels are similar among them and to other oxide spinels indicating a similar compressibility for this family of compounds independently of the Co valence and Co-Fe distribution between tetrahedral and octahedral sites.

Acknowledgements.

Financial support from the Spanish MINECO (Projects No. MAT2012-38213-C02-01) and Diputación General de Aragón (DGA-CAMRADS) is acknowledged. Authors would like to acknowledge the use of SAI from Universidad de Zaragoza. We also thank ALBA synchrotron for beam time allocation.

References.

[1] V. A. M. Brabers, in Hand Book of Magnetic Materials, edited by K. H. Buschow (North-Holland, Amsterdam, 1995), Vol. 8, p. 189

[2] D. Errandonea, 'AB_2O_4 Compounds at High Pressures' Ch2 in the book *Pressure-Induced Phase Transitions in AB_2X_4 Chalcogenide Compounds*, Springer Series in Materials Science 189, DOI: 10.1007/978-3-642-40367-5_2, Springer-Verlag Berlin Heidelberg 2014 E. Wiley.

[3] E. Greenberg, G. Kh. Rozenberg, W. Xu, R. Arielly, M. P. Pasternak, A. Melchior, G. Garbarino, L. S. Dubrovinsky et al., *High Press. Res.* 29 (2009) 764-779.

[4] T. Yamanaka A. Uchida and Y.Nakamoto, *Am. Miner.* 93 (2008) 1874-1881.

[5] Y. Ding, D. Haskel, S. G. Ovchinnikov, Y.-C. Tseng, Y. S. Orlov, J. C. Lang and H.-K Mao, *Phys. Rev. Lett.* 100 (2008) 045508.

[6] K. Schollenbruch, A. Woodland, D. Frost and F. Langenhorst, *High Press. Res.* 29 (2009) 520-524.

[7] G. Subías, V. Cuartero, J. García, J. Blasco, O. Mathon and S. Pascarelli, *J. Phys.: Conf. Ser.* 190 (2009) 012089.

[8] S. Ono, J. P. Brodholt, and G. D. Price, *Phys. Chem. Minerals* 33 (2006) 200-206.

[9] Y. Fei, D. J. Frost, H. K. Mao, C. T. Prewitt, and D. Häusermann, *Am. Mineral*. 84 (1999) 203-206.

[10] C. Haavik, S. Stolen,H. Fjellvag,M. Hanfland, and D.Häusermann, *Am. Mineral.* 85 (2000) 514-523.

[11] L. S. Dubrovinsky, N. A. Dubrovinskaia, C. McCammon, G. Kh. Rozenberg, R. Ahuja, J. M. Osorio-Guillen, V. Dmitriev, H.-P. Weber, T. Le Bihan, and B. Johansson, *J. Phys.: Condens. Matter* 15 (2003) 7697-7706.

[12] F. Baudelet, S. Pascarelli, O. Mathon, J. P. Itié, A. Polian and J. C. Chervin, *Phys. Rev. B* 82 (2010) 140412(R).

[13] G. Subías, V. Cuartero, J. García, J. Blasco, S. Lafuerza, S. Pascarelli, O. Mathon, C. Strohm, K. Nagai, M. Mito, and G. Garbarino, *Phys. Rev. B* 87 (2013) 094408.

[14] R. E. Cohen, I. I. Mazin, and D. G. Isaak, *Science* 275 (1997) 654-657.

[15] P. J. Murray and J. W. Linnet, *J. Phys. Chem. Solids* 37 (1975) 619-624.

[16] F. Fauth, I. Peral, C. Popescu, M. Knapp, *Powder Diffraction* 28 (2013) S360-S370.

[17] H. K. Mao, J. Xu, and P. M. Bell, *J. Geophys. Res*. 91 (1986) 4673-4676.

[18] A. P. Hammersley, S. O. Svensson, M. Hanfland, A. N. Fitch and D. Hausermann, *High Press. Res.* 14 (1996) 235-248.

[19] J. Rodríguez-Carvajal, *Physica B* 192 (1993) 55-69.

[20] Z. Wang, R. T. Downs, V. Pischedda, R. Shetty, S. K. Saxena, C. S. Zha, Y. S. Zhao, D. Schiferl, and A. Waskowska, *Phys. Rev B* 68 (2003) 094101.

[21] G. D. Rieck and G.D. Thijssen, *Acta Crystall. B* 24 (1968) 982-983.

[22] R. D. Shannon, *Acta Cryst. A*23 (1976) 751-767.

[23] R.J. Angel. M. Bujak, J. Zhao, G. Diego Gatta and S. D. Jacobsen, *J. Appl. Crystallogr*. 40 (2007) 26-32

[24] S. Klotz, J. C: Chervin, P. Munsch and G. Le Marchand, *J. Phys. D: Appl. Phys.* 42 (2009) 075413.

[25] F. D. Murnaghan *Proceedings of the National Academy of Sciences of the United States of America* 30 (1944) 244-247.

[26] F. Birch, *Phys. Rev.* 71 (1947) 809-824.

[27] S. Åsbrink, A. Waśkowska, L. Gerward, J. Staun Olsen, and E. Talik, *Phys. Rev. B* 60 (1999) 12651-12656.

[28] O. Gomis, J. A. Sans, R. Lacomba-Perales, D. Errandonea, Y. Meng, J. C. Chervin, and A. Polian, *Phy. Rev. B* 86 (2012) 054121.

[29] A. B. Garg, D. Errandonea, P. Rodriguez-Hernandez, S Lopez-Moreno, A. Munoz, C. Popescu, *J. Phys.: Condens. Matter* 26 (2014) 265402.

Figure Captions.

Figure 1. Rietveld refinement (λ=1.5418 Å) of $Co_{1.5}Fe_{1.5}O_4$ at ambient conditions (space group $Fd\bar{3}m$). Points and line stands for experimental and calculated patterns, respectively. The difference is plotted at the bottom together to the allowed reflections. Inset: Evolution of the cubic lattice parameter *vs.* Co-content in the $Co_xFe_{3-x}O_4$ series ($1 \leq x \leq 2$).

Figure 2. Powder x-ray diffraction patterns of $CoFe_2O_4$ (left) and $Co_{1.75}Fe_{1.25}O_4$ (right) at selected pressures. The asterisk marks the appearance of contribution from postspinel phase while cross indicate the vanishing spinel phase. The pressure was increased and released as indicated by arrows on the right of the picture.

Figure 3.- Pressure dependence of the unit cell volume per formula unit for (a) $CoFe_2O_4$, (b) $Co_{1.5}Fe_{1.5}O_4$ and (c) $Co_{1.75}Fe_{1.25}O_4$. Circles and squares stand for spinel and postspinel phases, respectively. Dark symbols: determination upon compression. Open symbols: determination upon decompression. The lines are guide for the eyes.

Figure 4.- Unit cell volume as a function of pressure for $Co_{1.5}Fe_{1.5}O_4$ and Co_2FeO_4. Continuous lines show the fits BM10 and BM23 for $Co_{1.5}Fe_{1.5}O_4$ and the fit BM23 for Co_2FeO_4. The broad arrow indicates the turning point in the pressure dependence of the cell volume for $Co_{1.5}Fe_{1.5}O_4$.

TABLES.

		Co_2FeO_4*		$Co_{1.75}Fe_{1.25}O_4$		$Co_{1.5}Fe_{1.5}O_4$		$CoFe_2O_4$	
Fit range		V_0 (Å^3)	K_0 (GPa)	V_0 (Å^3)	K_0 (GPa)	V_0 (Å^3)	K_0 (GPa)	V_0 (Å^3)	K_0 (GPa)
BM10	≤ 10 GPa	---	---	585.5 (7)	177(8)	576.4(6)	182(8)	584.9(3)	175(2)
BM23	≤ 23 GPa	560.9(1)	194.3(4)	576 (1)	247(14)	577(1)	209(9)	583(1)	250(12)

Table 1. Bulk modulus and reference volume according to the second order (K'=4) Birch-Murnaghan (BM) equation of state. BM10 and BM23 stand for the two ranges of fit indicated in the table. Numbers in parentheses refer to standard deviations of the last significant digits. (*) The values for this sample were calculated from the data of ref. 13 measured using He as pressure transmitting medium.

Figure 1.

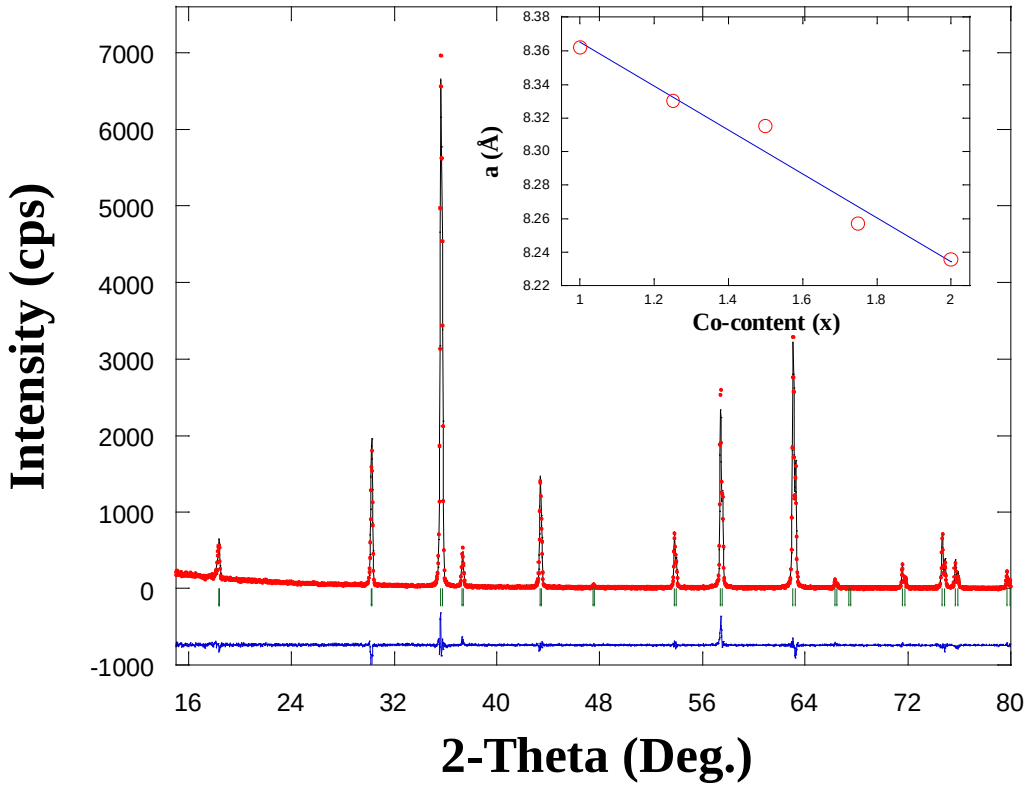
Intensity (cps)
7000
6000
5000
4000
3000
2000
1000
0
-1000
16
24
32
40
48
56
64
72
80
2-Theta (Deg.)
a (Å)
8.38
8.36
8.34
8.32
8.30
8.28
8.26
8.24
8.22
1
1.2
1.4
1.6
1.8
2
Co-content (x)

Figure 2.

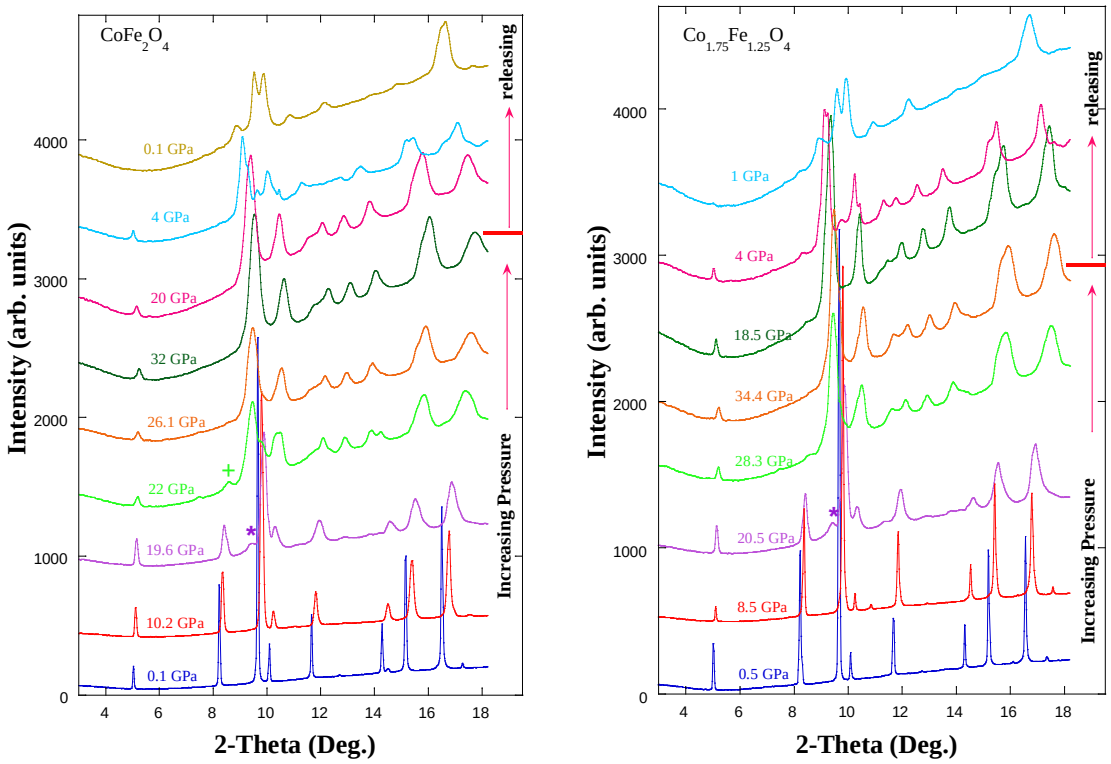
CoFe2O4
releasing
Increasing Pressure
0.1 GPa
4 GPa
20 GPa
32 GPa
26.1 GPa
22 GPa
19.6 GPa
10.2 GPa
0.1 GPa
Intensity (arb. units)
2-Theta (Deg.)
Co1.75Fe1.25O4
releasing
Increasing Pressure
1 GPa
4 GPa
18.5 GPa
34.4 GPa
28.3 GPa
20.5 GPa
8.5 GPa
0.5 GPa
Intensity (arb. units)
2-Theta (Deg.)

Figure 3.

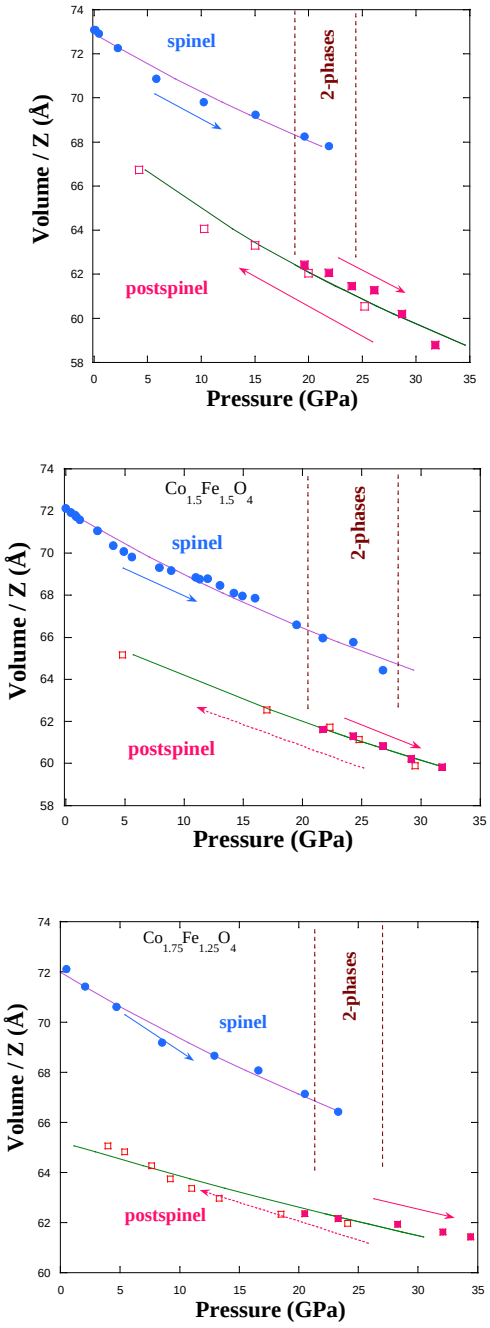
spinel
2-phases
postspinel
Volume / Z (Å)
Pressure (GPa)
Co1.5Fe1.5O4
spinel
2-phases
postspinel
Volume / Z (Å)
Pressure (GPa)
Co1.75Fe1.25O4
spinel
2-phases
postspinel
Volume / Z (Å)
Pressure (GPa)

Figure 4.